SEMARAK ILMU PUBLISHING

Journal of Advanced Research in Applied Sciences and Engineering Technology

Journal homepage:
https://semarakilmu.com.my/journals/index.php/applied_sciences_eng_tech/index
ISSN: 2462-1943

A Novel Slot-MIMO Antenna Approach for Improved Connectivity in Sub-6 GHz Applications

Menna Nabil[1,*], Hussein H. Ghouz[2], Sherif El-Diasty[2], Mohamed Edris[1]

[1] Department of Communications and Computers Engineering, The Higher Institute of Engineering, El-Shorouk City 11837, Egypt
[2] Department of Electronics and Communication Engineering, Arab Academy for Science, Technology & Maritime Transport, Giza Governorate 3650111, Egypt

ARTICLE INFO

Article history:
Received 19 December 2023
Received in revised form 1 July 2024
Accepted 15 July 2024
Available online 20 August 2024

Keywords:

5G; slot antenna; square slot; diamond slot; DGS; MIMO system; smartphone antenna

ABSTRACT

This paper presents a proposed Slot-MIMO antenna with two identical ports, each port is fed through 50-Ohm microstrip line to operate within the sub-6 GHz (3.5-4.5 GHz) for fifth-generation (5G) cellular phone applications. The proposed MIMO antenna has been designed on FR-4 dielectric substrate (ε = 4.4, δ = 0.025, and h = 1.6 mm). The ground has two basic slots, one square slot radiator, and one irregular square slot radiator filled with a Diamond conductor shape. In addition, the ground has a DGS structure (8-slots) beside the two basic slots. The ground DGS is used to adjust the resonance frequency as well as to reduce the mutual coupling between the ports. The simulated result indicated that the proposed MIMO antenna has a gain of about 2.5 dBi and an impedance bandwidth of 614 MHz at the -10-dB (3.751-4.365 GHz). However, an impedance bandwidth of 1180 MHz at -6-dB (3.32-4.5 GHz) is achieved. The mutual coupling is less than -24 dB overall the bandwidth, and the efficiency is more than 80% at the antenna resonance frequency (4.15 GHz). This antenna has been implemented and measured, and the results have been agreed with the simulated ones. In addition, the proposed Slot-MIMO antenna can be used as a MIMO antenna-cell with the smartphone. Many MIMO cells can be etched on the smartphone motherboard to improve connectivity with high isolation.

1. Introduction

The fifth-generation wireless technology (5G) requires a compact antenna, commonly called a 5G antenna. It is essential for enabling higher data rates and interaction between 5G-capable devices and the network infrastructure [1,2]. Compared to their forerunners, such as 4G antennas, these antennas have been designed to operate at substantially higher frequencies [3,4]. The 5G antennas for the lower band (Sub-6 GHz) are an integral part of the next-generation wireless communication networks. These antennas, which typically operate in the lower frequency bands below 6 GHz, are essential for giving users extensive coverage and reliable connectivity. Lower band 5G antennas are preferable for enabling seamless connectivity in urban locations and indoor situations because they

* *Corresponding author.*
E-mail address: mennamorad2012@gmail.com

https://doi.org/10.37934/araset.50.2.103118

can transport signals over greater distances and cut through obstructions more effectively than their higher-frequency equivalents. The sub-6 GHz spectrum, which covers frequencies around 600 MHz, 2.5 GHz, 3.5 GHz, and 5 GHz, is one of the 5G frequency bands that these antennas are made to accommodate. By utilizing these lower frequencies, the fifth-generation networks can guarantee better signal propagation, more capacity, and improved network performance. To create a comprehensive 5G infrastructure that can meet the rising demand for high-data speed, improved mobile broadband services, and developing Internet of Things (IoT) applications, the deployment of lower band 5G antennas is the first crucial step. Manufacturers of lower band 5G antennas are constantly coming out with innovative antenna designs that are compact in size and effective, and can be easily incorporated into a variety of infrastructure and devices, including smartphones, base stations, and small cells. With the widespread use of 5G technology, the installation of these antennas will be crucial in changing how we communicate and engage in the digital age and opening the door to cutting-edge new applications that will influence our future.

Modern wireless communication systems frequently include a type of printed antenna known as a slot antenna. A metallic radiating slot and a ground plane are what make up the small, low-profile antenna, and they are separated by a dielectric substrate [5,6]. The radiating slot normally has a rectangular or circular shape, and the dimensions of the slot play a crucial role in defining the operating frequency and other features of the antenna's performance [7,8]. Between the radiating slot and the ground plane, the dielectric substrate employed in slot antennas acts as both mechanical support and electrical isolation. This substrate can be constructed from a variety of substances, including ceramic, FR-4, and Rogers, each of which has a unique dielectric constant that affects the performance of the antenna. Slot antennas provide several benefits, including being lightweight, inexpensive, and simple to fabricate using conventional printed circuit board (PCB) techniques [9,10]. They are frequently used in mobile devices, satellite communications, Wi-Fi routers, and many other applications due to their planar shape, which allows easy integration with other electronics [11]. The comparatively low gain of slot antennas in comparison to other antenna types, such as parabolic or horn antennas, is one of their drawbacks [12]. However, they are appealing options for a variety of wireless communication applications where size and cost considerations are important because of their tiny size and ease of integration. To maintain the viability of slot antennas in the constantly changing context of contemporary wireless communication systems, researchers and engineers continue to investigate novel designs and ways to enhance the gain and performance of slot antennas [13]. Overall, due to its adaptability, compactness, and integration abilities, slot antennas have emerged as a prominent option in wireless communication systems.

To improve the performance of an antenna, a rectangular-shaped DGS is a vital element frequently used in antenna design. The DGS typically has a rectangular pattern that is etched into the ground plane. This structure's main job is to block out-of-band surface waves and enhance the gain, directivity, and impedance matching of the antenna's radiation output [14,15]. An electromagnetic barrier that serves as a stopband for surface waves is created by carefully placing a rectangular DGS beneath the antenna's radiating element, stopping their propagation and minimizing their detrimental impacts on the antenna's performance [16]. As a result, cross-polarization is decreased, radiation efficiency is increased, and antenna gain is increased. Furthermore, the rectangular DGS makes it simpler to produce a desired frequency response and impedance matching by enabling better control over the antenna's resonance frequency and bandwidth. In array arrangements, it also helps to lessen mutual coupling between antenna parts, improving array performance and minimizing interference. In finality, a rectangular-shaped DGS is essential for antenna design because it enhances radiation characteristics, reduces surface waves, and offers better frequency management, all of which improve antenna performance and system effectiveness.

A leading supplier of electromagnetic simulation software with a focus on antenna design and analysis is Computer Simulation Technology (CST). Researchers and engineers now approach antenna design and optimization in a completely new way by using CST's antenna simulation tools. CST has made it possible to create cutting-edge antenna systems that can meet the rising demands of contemporary wireless and communication technologies by leveraging the power of computer simulation. Engineers can precisely model and simulate a variety of antennas, including dipole, patch, helical, Yagi-Uda, phased array, and many others, using CST's antenna simulation software. The software's user-friendly interface enables intuitive design and parameterization and is used by both experienced designers and amateurs. The innovative electromagnetic solver at the centre of CST's antenna simulation uses numerical techniques to solve Maxwell's equations and successfully predicts the behaviour of electromagnetic waves in intricate antenna configurations. This solver incorporates several practical elements, including material characteristics, radiation patterns, impedance matching, and coupling effects, giving engineers crucial knowledge about how well their antenna designs function. The ability to swiftly iterate and optimize antenna designs without the need for expensive and time-consuming physical prototypes is one of the main benefits of adopting CST's antenna simulation. Engineers can quickly see the effects of changing parameters on antenna performance, like antenna dimensions, materials, and feeding schemes. CST's software makes sure that the antennas are effective, dependable, and fulfil the exacting standards of contemporary wireless communication, whether they are being designed for 5G networks, satellite communication, radar systems, or radio-frequency identification (RFID). Overall, antenna simulation software from CST is essential for enabling engineers to design advanced, effective antennas. CST continues to enhance antenna technology by providing a full range of tools and precise numerical solvers, which contributes to the constant connectivity and communication that characterize our contemporary environment. Investigating antenna properties and determining the best structure for the antenna required the use of CST software [17]. Recently, many designs for smartphone antennas for 5G applications have been provided at the frequency range below 6 GHz [18-35].

In this paper, a Slot-MIMO antenna is proposed, designed, simulated, optimized, and measured. The paper is organized into four sections. The second section presents the proposed Slot-MIMO antenna describing its structure, materials, and operating principles. The third section presents design steps and parametric study in detail of the process undertaken to optimize the performance of the proposed antenna. This includes resonance frequency, bandwidth, and isolation between antenna ports. The fourth section presents results analysis and measurement to rigorously examine the simulation and measurement results to give insights into the performance validation of the proposed antenna. Finally, the paper is concluded with a conclusion section.

2. The Proposed Slot-MIMO Antenna

The current smartphone specifications including lightweight, compact design, and integration with RF circuits are challenges to the designers to achieve high performance, high isolation between ports, and good connectivity. In our proposed design a slot antenna has been selected due to its easy fabrication on the motherboard. The goal of the proposed design is to achieve the smartphone specifications.

The proposed Slot-MIMO antenna is shown in Figure 1. The top layer consists of a pair of 50Ω microstrip lines feed and two circular rings. The bottom layer consists of two basic slots, one square slot radiator, and one irregular square slot radiator (Diamond). In addition, a DGS is used beside the two basic slot radiators.

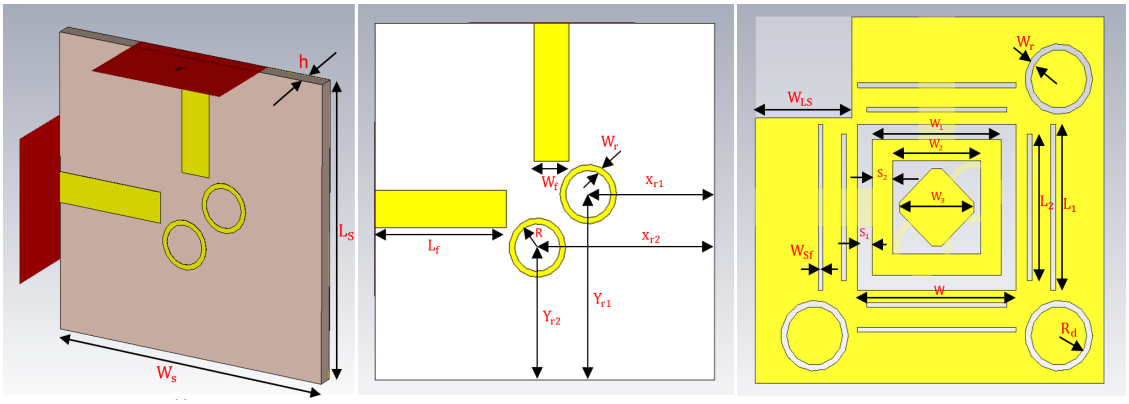

(a) (b) (c)

Fig. 1. The proposed slot antenna configuration, (a) 3D-view, (b) top, and (c) bottom

Table 1, summarizes the list of optimized parameter values for the proposed slot-MIMO antenna. This antenna is simulated using CST studio to evaluate its performance.

Table 1
The optimum dimensions of the proposed slot MIMO antenna

Parameter	Value(mm)	Parameter	Value(mm)	Parameter	Value(mm)	Parameter	Value(mm)
$W_S = L_S$	*30*	L_1	*13.6*	W_{LS}	*8.3*	W_r	*0.5*
W	*13.6*	L_2	*12*	R_d	*2.4*	$X_{r1} = Y_{r2}$	*10.6*
W_1	*11.1*	S_1	*1.25*	L_f	*11.6*	$Y_{r1} = X_{r2}$	*15.25*
W_2	*7.6*	S_2	*1.75*	W_f	*3.11*	t	*0.035*
W_3	*6.35*	W_{sf}	*0.4*	R	*2*	h	*1.6*

The proposed antenna is fabricated on FR-4 dielectric substrate as shown in Figure 2.

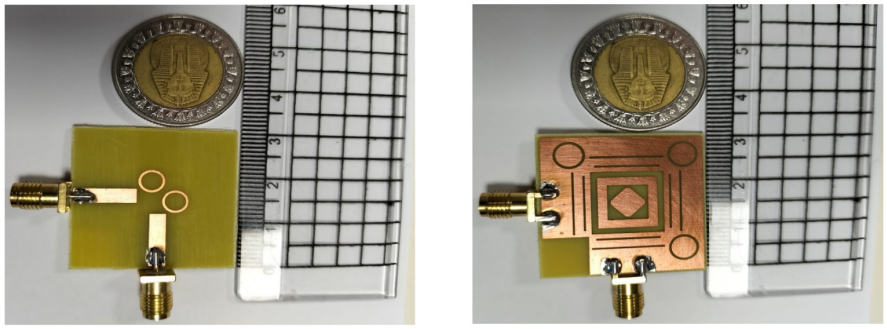

(a) (b)

Fig. 2. Fabricated antenna, (a) top view and (b) bottom view

The optimized simulated results including S-parameters, gain, VSWR, efficiency, and radiation patterns are presented in Figure 3 through Figure 5 along with the measured result. The proposed Slot-MIMO antenna satisfied the specifications mentioned above.

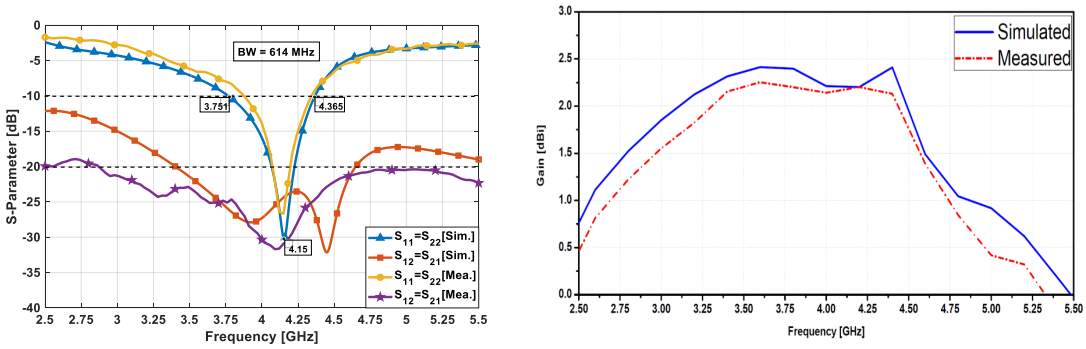

(a) (b)

Fig. 3. Measured and simulated (a) S-parameters, and (b) gain of the proposed slot antenna

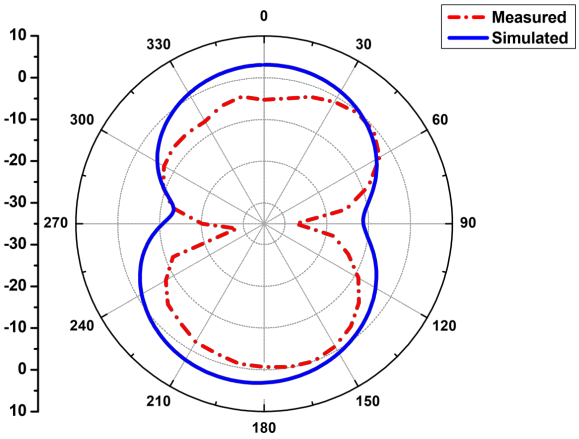

Fig. 4. Measured and simulated antenna radiation patterns

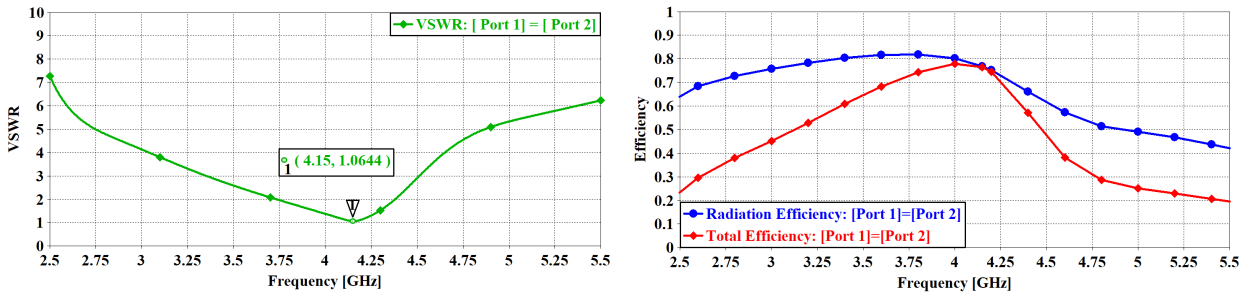

(a) (b)

Fig. 5. (a) Voltage standing wave ratio, and (b) Efficiency of the proposed slot antenna

3. Design Steps and Parametric Study

The design is carried out in a variety of steps using the CST Studio simulator. These steps include the effects of the rectangular square slot, the irregular square slot, the pair of parasitic circular rings, the ground corner cut, and the ground DGS including multi slots (slots under the feeder and slots in front of the feeder). These steps are presented in Figure 6(a) through Figure 6(e).

Practically, in antenna design and implementation, a variety of substrates with different permittivity and tangent loss are available. In our proposed design, the FR-4 substrate is selected due to its low cost and wide use. However, it has a high tangent loss and moderate permittivity. The proposed antenna is designed, investigated, evaluated, and optimized on the assumed substrate.

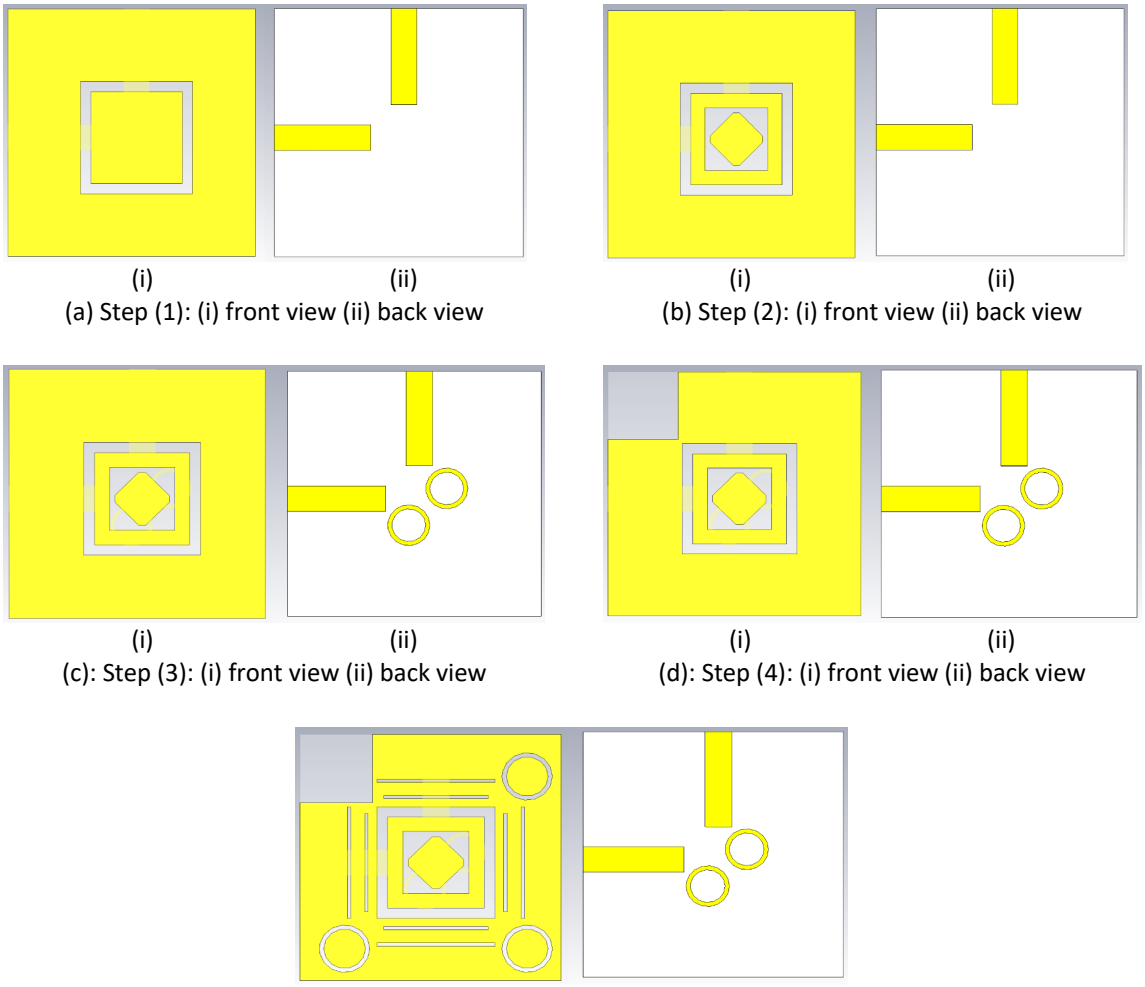

(i) (ii)
(a) Step (1): (i) front view (ii) back view

(i) (ii)
(b) Step (2): (i) front view (ii) back view

(i) (ii)
(c): Step (3): (i) front view (ii) back view

(i) (ii)
(d): Step (4): (i) front view (ii) back view

(i) (ii)
(e): Step (5): (i) front view (ii) back view

Fig. 6. Design steps of the proposed slot MIMO antenna

The first step (initial step) is to optimize the dimensions of the square slot for the required antenna resonance. The results of the parametric study are presented in Figure 7. It is clear from the results (Figure 7(a)) that the width of the single slot S_1 = 1.25 mm closely matches the required antenna resonance (4.212 GHz). Therefore, the value S_1 = 1.25 mm is selected for our antenna design. The mutual coupling (Figure 7(b)) varies for different slot widths.

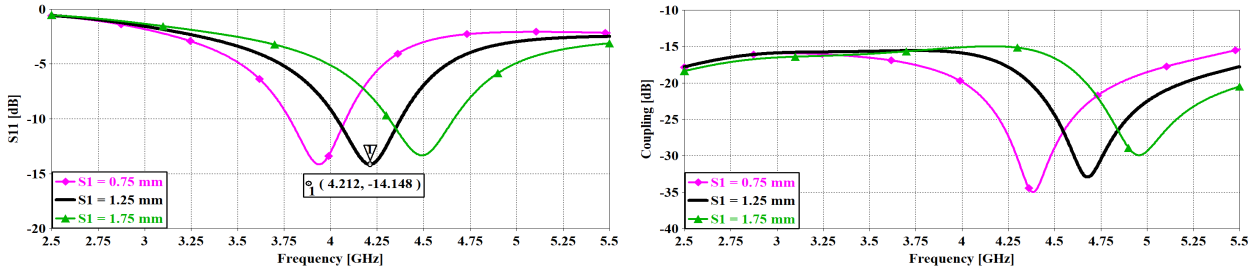

(a) (b)

Fig. 7. S-parameter results for the parametric study of the first step (different values of S_1), (a) S_{11} and (b) S_{21}

To fine-adjust the required resonance at 4.15 GHz, a second step is carried out by adding an additional square slot filled with a diamond conductor shape as presented in Figure 8(b).

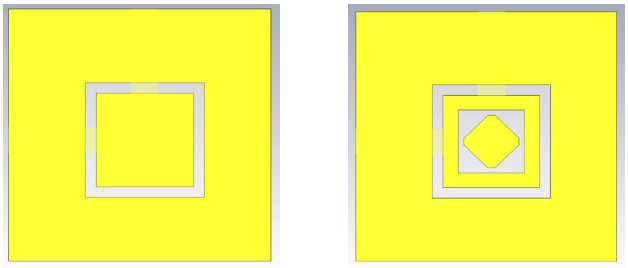

(a) (b)

Fig. 8. The second ground slot: (a) single square slot (b) irregular square slot (diamond)

The effect of the second slot is to restore the antenna resonance at 4.112 GHz instead of 4.212 GHz as it is clear from Figure 9.

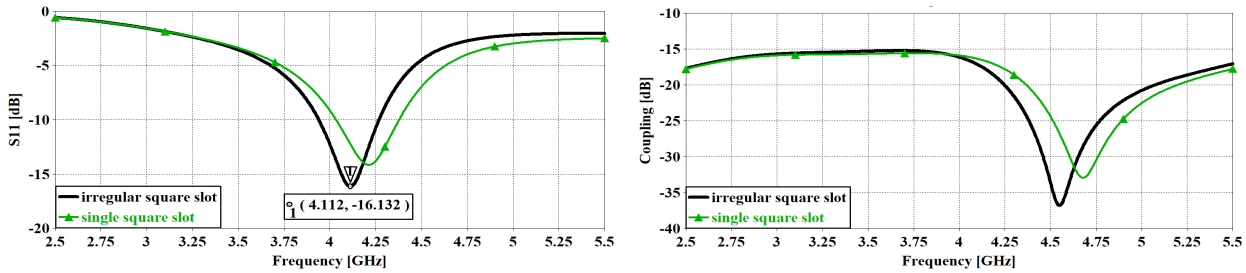

(a) (b)

Fig. 9. The antenna S-parameter results for different ground two slots, (a) S_{11} and (b) S_{21}

In the third step, to reduce the mutual coupling between ports, a pair of parasitic circular rings have been used across the square slot as presented in Figure 10. The antenna bandwidth is equal to 360 MHz, the antenna reflection coefficient is equal to -16.8 and the mutual coupling is equal to -19 dB as presented in Figure 9 for last parametric step. In Figure 10(b), the configurations of the various ring positions, radius, and thickness are simulated and investigated.

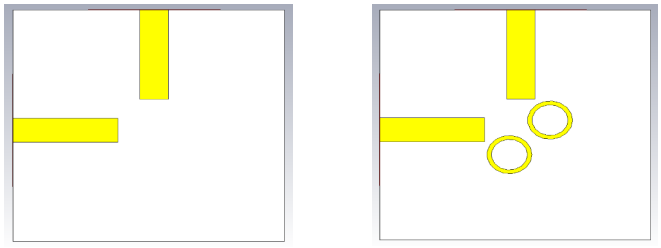

(a) (b)

Fig. 10. (a) Without parasitic circular ring, and (b) With pair of parasitic circular ring

In Figure 11, the simulated S-parameters for a microstrip-fed square-ring slot antenna (Figure 10(a)), and the antenna with a pair of parasitic circular rings (Figure 10(b)) are evaluated and compared. As shown, for the antenna with varied ports, the desired impedance bandwidth improved from 0.335 to 0.345 GHz by using the proposed parasitic rings. Also, the mutual coupling reduced from -17.8 dB to -19.1 dB.

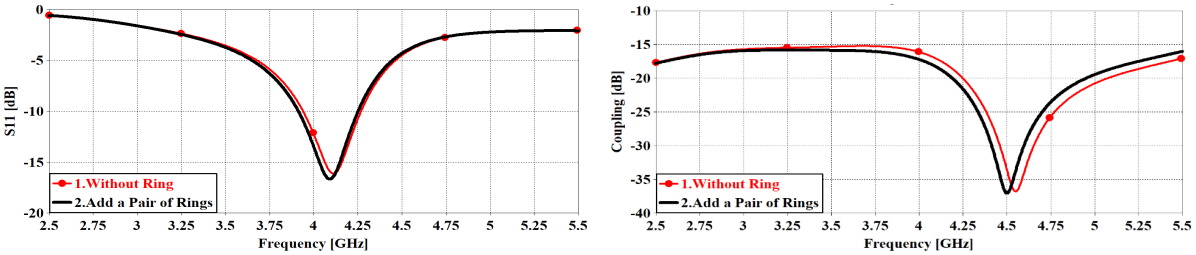

(a) (b)

Fig. 11. S-parameter results for the various designs illustrated in Figure 10, (a) S_{11} and (b) S_{21}

Figure 12 presented the simulated S-parameters for various placements of the parasitic circular rings across the square resonator. As shown, the position of the parasitic circular rings has a significant impact on the antenna frequency response. The ring position at ($X_{r1} = Y_{r2}$ = 11.5 mm) is the optimum position for the desired frequency range (3.9 - 4.25 GHz).

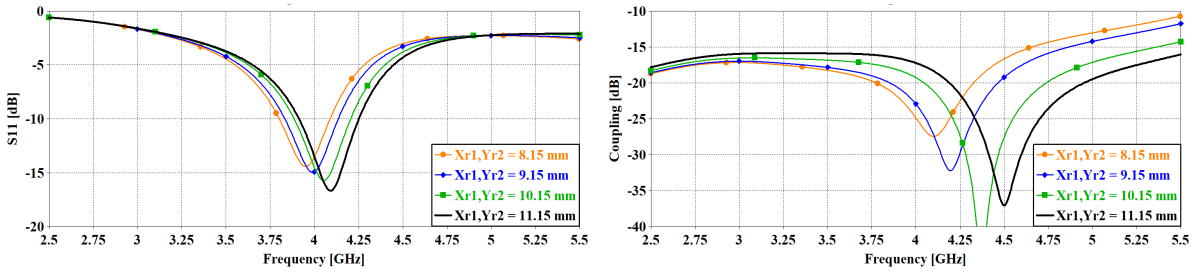

(a) (b)

Fig. 12. The antenna S-parameter results for different ring positions ($X_{r1} = Y_{r2}$), (a) S_{11} and (b) S_{21}

Figure 13 presented the S-parameter for various values of the parasitic circular ring radius (R). Their radius can have an impact on the operation frequency. The effects of (R) on the resonance frequency are shown in Figure 13(a), when the size reduces from 2.5 to 2 mm the antenna resonance changes from 4.06 to 4.09 GHz. The ring radius at (R = 2 mm) is the optimum ring radius.

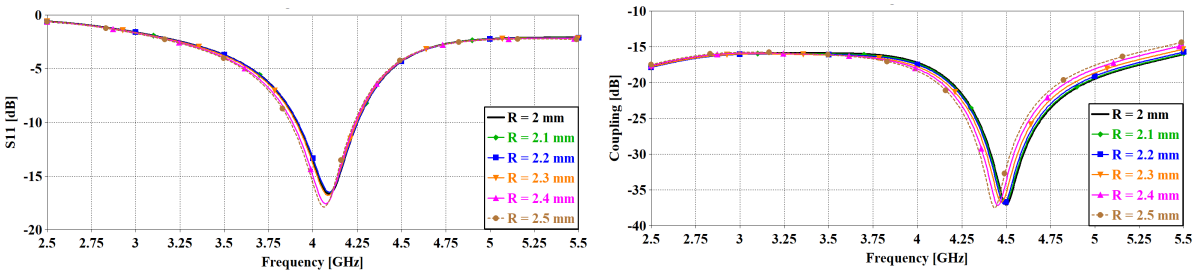

(a) (b)

Fig. 13. The antenna S-parameter results for different ring radius R, (a) S_{11} and (b) S_{21}

Figure 14 presented the simulated S-parameters for various widths of the ring (W_r). Figure 14(a) illustrates the impacts of (W_r) to adjust the response frequency, where the antenna resonance shifts from 4.05 to 4.1 GHz as the size decreases from 1 to 0.5 mm. The ring width at (W_r = 0.5 mm) is the optimum ring width.

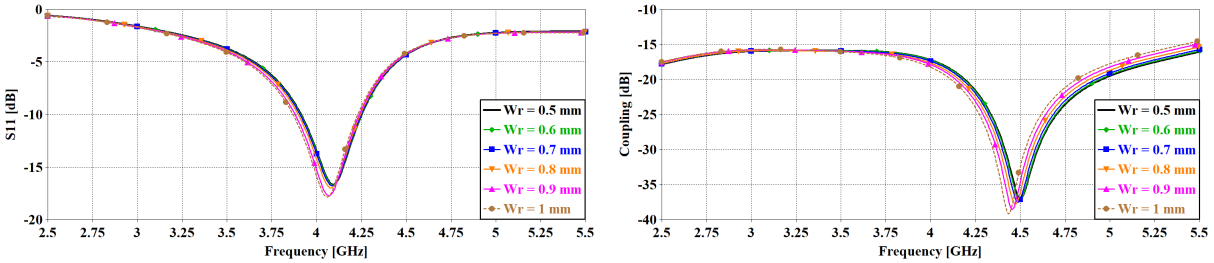

(a) (b)

Fig. 14. The antenna S-parameter results for different ring thicknesses W_r, (a) S_{11} and (b) S_{21}

The mutual coupling between ports is partially minimized using the cut edge of the ground as previously presented in Figure 6(d). The results of the parametric study for the fourth step are presented in Figure 15. Minimum mutual coupling is achieved over the antenna bandwidth while maintaining the same resonance frequency (W_{LS} = 8.3 mm) as compared to the case without a ground cut (W_{LS} = 0.0 mm) as presented in Figure 15(b).

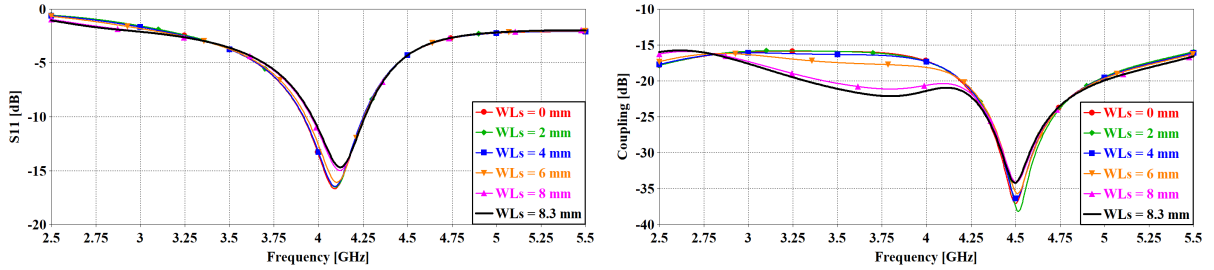

(a) (b)

Fig. 15. The S-parameter results for different values of cut edge W_{LS}, (a) S_{11} and (b) S_{21}

The final step is to use a DGS technique to enhance the proposed antenna bandwidth and mutual coupling. Three circular rings and two pairs of four slots are etched on the ground to enhance the antenna bandwidth and the mutual coupling.

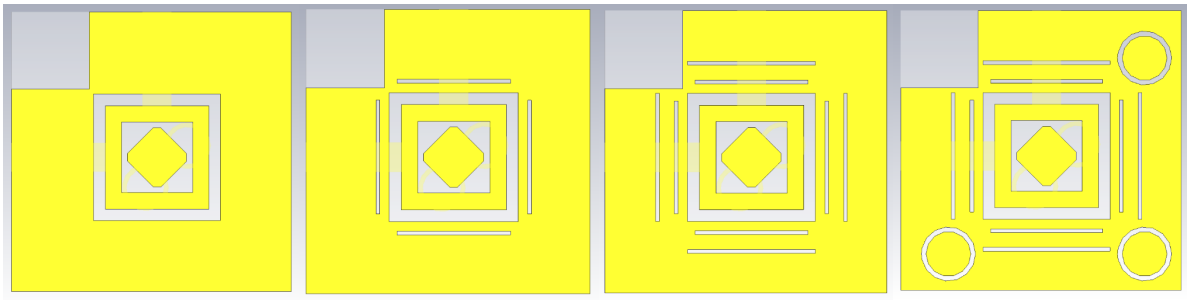

(a) (b) (c) (d)

Fig. 16. (a) Without ground DGS, (b) With the first group of slots (DGS1), (c) DGS1 and the second group of slots (DGS2), (d) DGS1 and DGS2 with three parasitic circular rings

It is clear that the antenna resonance is enhanced from -15 dB to -30 dB as depicted in Figure 17(a). Also, the bandwidth (at -10dB) of the proposed antenna is increased from 564.0 MHz to 614.0 MHz, increment by about (50.0 MHz) as presented in Figure 17(a). Moreover, the mutual coupling is also enhanced as presented in Figure 17(b) (Black curve).

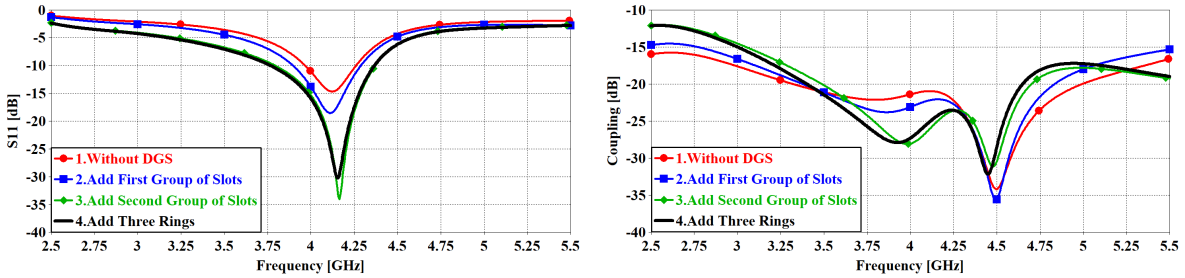

(a) (b)

Fig. 17. The S-parameter for the final design step illustrated in Figure 16, (a) S_{11} and (b) S_{21}

The Final parametric study results for the different design steps presented in Figure 6, are compared and plotted together in Figure 18. The optimum dimensions of the proposed Slot-MIMO antenna are presented previously in Table 1.

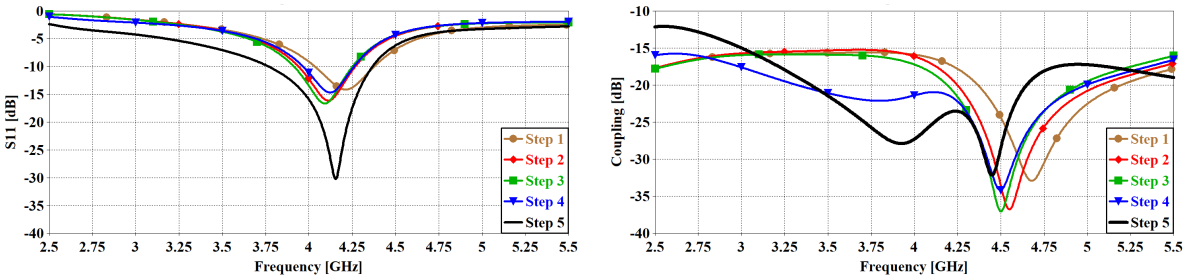

(a) (b)

Fig. 18. S-parameter for the design steps of the proposed slot-MIMO antenna, (a) S_{11} and (b) S_{21}

4. Results Analysis and Measurement

The S-parameters for the proposed Slot-MIMO antenna are shown previously in Figure 3(a). It is evident that the antenna offers 614 impedance bandwidth (3.751-4.365 GHz) for S_{11} ≤-10 dB. In addition, the mutual coupling between ports is less than -24 dB at the resonance frequency (4.15 GHz). Figure 3(b) illustrates the antenna maximum gain of about 2.5 dBi.

The Voltage Standing Wave Ratio (VSWR) is a critical statistic for determining antenna performance. The proposed antenna achieved a VSWR of 1.0644 at the resonance frequency as shown in Figure 5(a). Radiation and total efficiencies are presented in Figure 5(b). Despite being designed on FR-4 dielectric substrate, the proposed antenna achieved at the operational frequency (4.15 GHz) maximum efficiency of 80%.

The current density distribution on a slot antenna depends on various factors including the dimensions of the slot, the frequency of operation, and the feeding mechanism. Figure 19 shows the current densities at the resonant frequency (4.15 GHz) in the top and bottom layers respectively. As shown, there is a significant current distribution around the square slot radiator and the DGS slots in the ground plane. It has increased at the edges of the slot while it has decreased towards the slot radiator centre. It can be seen for the different feeding ports, the currents flow contrary to each other. In addition, the employed parasitic circular rings have low current densities.

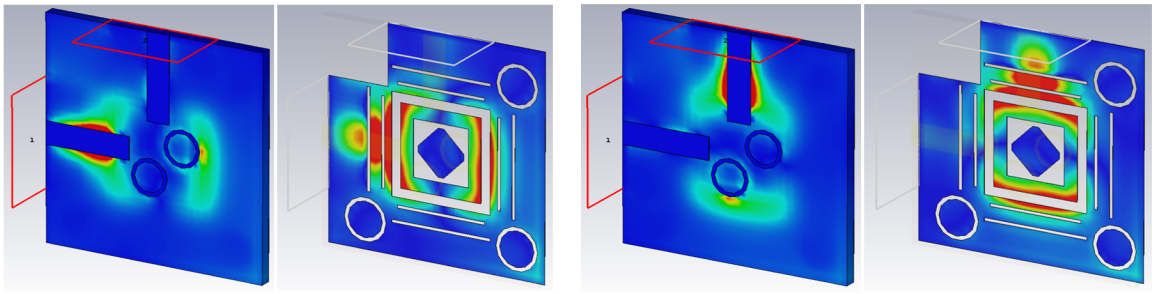

(a) (b)

Fig. 19. Current densities at 4.15 GHz for (a) Port 1 and (b) Port 2

It's important to note that the size and form of the slot, the dielectric material employed, the feeding technique, and the presence of any additional structures or elements close to the antenna can all have an impact on the shape and properties of the radiation pattern. Figure 20 shows the 2D-polar radiation patterns of the antenna at 4.15 GHz.

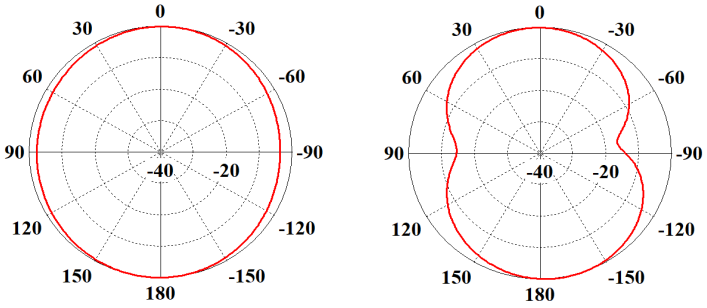

(a) (b)

Fig. 20. 2D-polar radiation patterns for (a) H-plane and (b) E-plane

Figure 21 shows the antenna's 3D radiation patterns when it is fed in a different way (Port 1 and Port 2). The antenna displays comparable radiation patterns, as can be observed. As can be seen, the slot antenna's radiation patterns are meant to resemble dumbbells and are appropriate for covering the top and bottom of the smartphone PCB, increasing the radiation coverage of the 5G antenna design. As a result, antenna designers meticulously craft the dimensions and arrangement of the slot to create the appropriate radiation pattern for individual purposes.

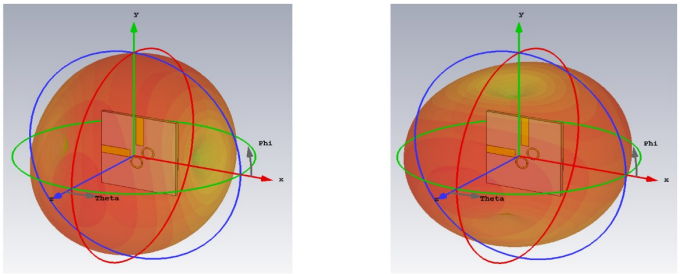

(a) (b)

Fig. 21. 3D Transparent schematic of the antenna radiation patterns: (a) port 1 and (b) port 2

The antenna prototype was carefully created using strict design guidelines. To ensure that the dimensions and material choices were accurate, the construction procedure required meticulous

attention to detail. The antenna underwent a thorough testing process when it was finished to assess its performance. The S-parameters, an important set of measurements in the field of antenna engineering, were the main focus of this testing. These S-parameters gave important information about the interaction between the antenna and the electromagnetic signals it is intended to transmit or receive. A prototype of the design was fabricated, and its S-parameters were tested. A proposed slot antenna prototype was fabricated as shown in Figure 2.

The network analyser was crucial to our antenna testing process since it was used to painstakingly measure the antenna's S-parameters. This critical stage enabled us to evaluate the antenna's performance traits across a range of frequency bands, including its impedance, reflection coefficient, and transmission coefficient. We were able to obtain a lot about how the antenna interacted with the surroundings and how effectively it transmitted and received signals by taking precise S-parameter measurements. The network analyser became an essential instrument in our research and development activities as a result of these findings, which provided the fundamental foundation for refining the antenna's design and guaranteeing its efficacy in practical implementations. The measurement settings for the antenna S-parameter are shown in Figure 22(a). As can be observed, the network analyser was used to measure the S-parameters of the antenna, including S_{11} /S_{22} and S_{21}/S_{12} characteristics.

The anechoic chamber was a crucial instrument for accurately determining the slot antenna's radiation pattern. The chamber offered a setting that was essentially free of outside influence due to its walls' painstaking design to absorb and reduce electromagnetic wave reflections. The measurements were accurate and faithful to the performance of the antenna by way of the controlled environment. The slot antenna was placed inside the chamber on a precise testing apparatus and meticulously aligned for best alignment. The radiation parameters of the antenna at various angles and frequencies were captured using a customized antenna measurement device outfitted with high-frequency probes and receivers. We were able to create a thorough radiation pattern that showed how the antenna transmitted electromagnetic energy in three-dimensional space by rotating the antenna and gathering data at various spots. The measurement sets for the radiation properties are shown in Figure 22(b). The anechoic chamber was used to measure the antenna radiation pattern, as seen.

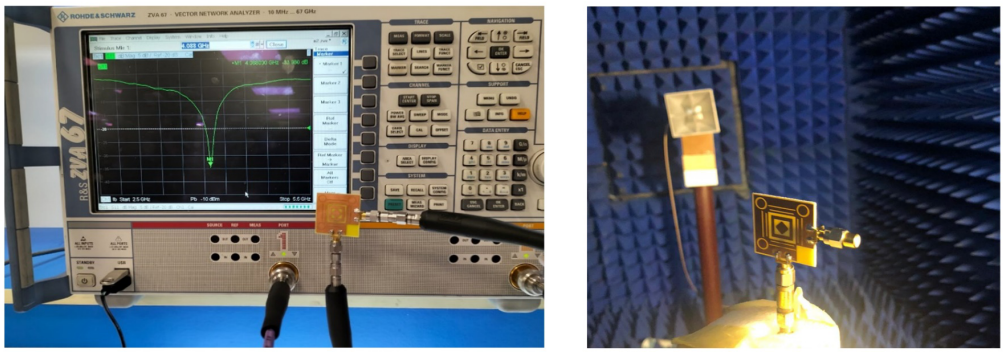

(a) (b)

Fig. 22. Measurement setup: (a) S-parameter and (b) Radiation pattern

Figure 3(a) shows the prototype's measured S-parameter results. As shown, the antenna offers excellent impedance matching at 4.15 GHz (centre frequency of the desired frequency band). For the manufactured sample, high isolation with less than -24 dB mutual coupling was attained. Additionally, it can be confirmed that there is a good agreement between them when compared to the simulations.

The measured and simulated radiation patterns of the fabricated prototype at 4.15 GHz are shown in Figure 4. As seen, the measured exhibits desirable radiation that agrees well with the simulations. Figure 3(b) displays the simulation and measurement results for the antenna gain versus frequency. The agreement between simulation and measurement is also quite good.

The performance comparison between the proposed Slot-MIMO antenna and the antenna that has been published in the literature is shown in Table 2. There is a discussion of fundamental properties like bandwidth, efficiency, and gain. With sufficient characteristics, it can be seen that the proposed design can achieve better performance. The proposed antenna, in contrast to the majority of the known 5G antenna designs, is planar, easy to integrate, and offers a pattern with full radiation coverage supporting various sides of the mobile phone PCB. It also displays a wider bandwidth. High gains and radiation/total efficiencies are also provided.

Table 2
Comparison between the presented and recently reported 5G mobile phone antennas

Reference	Antenna Type	Resonance Frequency(GHz)	Bandwidth (GHz)	Efficiency (%)	Gain (dBi)	Antenna Element (mm^2)	Isolation (dB)
[18]	symmetric dipole antenna	3.5	3.4-3.6	48-67	–	23.2×5.6	16
[19]	L-shaped metal strips	3.5	3.42-3.69	52.7-60.5	–	16×6	24
[20]	Dual-band antenna	3.5/5	3.1-3.6/4.4-6.1	50-65/65-75	5.8	5.77×18	18.5
[21]	shorted loop antenna	3.5	3.4-3.6	65	4.2-5.9	6×6.5	10
[22]	Coaxial-Fed Patch	4.7	4.4-5	40-80	5.5	–	12
[23]	H-shaped monopole	3.5	3.4–3.6	42-65	2.87	12.5×18.5	12
[24]	I-shaped grounding F-type antenna	4.5	3.68-5.27	–	4.5	–	15
[25]	L-shaped monopole	3.5	3.4-3.6	50-75	4	4.6×5.6	15
[26]	Fractal Monopole	3.5	3.4-3.6	65-75	–	–	12.2
[27]	Slot and Loop	3.5	3.4-3.6	42-73	1.6-4.5	27.3×1.2/26.5×1	15
[28]	balanced open-slot antenna	3.5	3.4-3.6	62-76	3.5	3×21.5	17.5
[29]	slot antenna	3.6	3.4-3.8	55-70	3	30×30	25
[30]	slot-patch antennas	3.6	3.55-3.65	52-76	4.5-6.2	–	11
[31]	T-shaped feeding element, an inverted U-shaped radiating element	3.5	3.4-3.6	60-70	–	17.4×6	20
[32]	inverted-F antennas	3.5	3.4-3.6	–	2.7-3.9	–	20
[33]	loop antennas	3.5	3.4-3.6	35-50	2	9.4×14.2	15
[34]	open-end slots and a QMSIW antenna.	3.5	3.4-3.6	50-80	–	17×17	12.5
[35]	novel compact tightly arranged pairs monopole	3.5	3.4-3.6	49-61	–	12×7	17

Proposed	and an edge-fed dipole Slot_MIMO	4.15	3.751-4.365	80	2.5	30×30	24

5. Conclusions

A proposed Slot-MIMO antenna has been designed, simulated, optimized, and presented in this paper. The resonance frequency for the proposed antenna is 4.15 GHz, with a wide bandwidth from 3.751 to 4.365 GHz at -10 dB level. The mutual coupling between ports is less than -24 dB, and the maximum gain is approximately 2.5dBi at the resonance frequency. The antenna efficiency is 80%, and the VSWR is about 1.0644 over the band. In addition, the proposed Slot-MIMO antenna has been fabricated on FR-4 dielectric substrate and tested. Good agreement has been obtained between simulated and measured results. Based on these results, the presented antenna achieved the current specifications of the smartphone needs. Thus, the proposed MIMO antenna can be integrated with smartphone motherboard as many different MIMO-Cells to improve connectivity in the sub-6 GHz band providing high isolation at the desired resonance frequency.

Acknowledgement
This research was not funded by any grant.

References
[1] Rashmitha, R., N. Niran, Abhinandan Ajit Jugale, and Mohammed Riyaz Ahmed. "Microstrip patch antenna design for fixed mobile and satellite 5G communications." *Procedia Computer Science* 171 (2020): 2073-2079. https://doi.org/10.1016/j.procs.2020.04.223

[2] Abirami, M. "A review of patch antenna design for 5G." In *2017 IEEE International Conference on Electrical, Instrumentation and Communication Engineering (ICEICE)*, pp. 1-3. IEEE, 2017. https://doi.org/10.1109/ICEICE.2017.8191842

[3] El-Wazzan, Marwa M., Hussein H. Ghouz, Sherif K. El-Diasty, and Mohamed A. Aboul-Dahab. "Compact and integrated microstrip antenna modules for mm-wave and microwave bands applications." *IEEE Access* 10 (2022): 70724-70736. https://doi.org/10.1109/ACCESS.2022.3187035

[4] Ghouz, Hussein Hamed. "Novel compact and dual-broadband microstrip MIMO antennas for wireless applications." *Progress In Electromagnetics Research B* 63 (2015): 107-121. https://doi.org/10.2528/PIERB15051304

[5] Abdullah, RSA Raja, D. Yoharaaj, and A. Ismail. "Bandwidth enhancement for microstrip antenna in wireless applications." *Modern Applied Science* 2, no. 6 (2008): 179-187. https://doi.org/10.5539/mas.v2n6p179

[6] Srisuji, T., and C. Nandagopal. "Analysis on microstrip patch antennas for wireless communication." In *2015 2nd International Conference on Electronics and Communication Systems (ICECS)*, pp. 538-541. IEEE, 2015. https://doi.org/10.1109/ECS.2015.7124965

[7] Al-hetar, Abdulaziz M., and Esmat AM Aqlan. "High performance & compact size of microstrip antenna for 5G applications." In *2021 International Conference of Technology, Science and Administration (ICTSA)*, pp. 1-3. IEEE, 2021. https://doi.org/10.1109/ICTSA52017.2021.9406537

[8] Veerendra, K., G. Padma Ratna, and S. Nagakishore Bhavanam. "Design of microstrip patch antenna with parasitic elements for wideband applications." *International Journal Of Innovative Research In Technology* 6, no. 2 (2019): 324-327.

[9] Stanley, Manoj, Yi Huang, Hanyang Wang, Hai Zhou, Ahmed Alieldin, Sumin Joseph, Chaoyun Song, and Tianyuan Jia. "A dual-band dual-polarised stacked patch antenna for 28 GHz and 39 GHz 5G millimetre-wave communication." In *2019 13th European Conference on Antennas and Propagation (EuCAP)*, pp. 1-4. IEEE, 2019.

[10] Swelam, W., N. Rashad, and M. H. Abd ElAzeem. "Millimetric Broadband Ankh Key Antenna for 5G Applications." *Journal of Advanced Research in Applied Mechanics* 42, no. 1 (2018): 7-11.

[11] Ghouz, Hussein Hamed Mahmoud, Mohamed Fathy Abo Sree, and Muhammad Aly Ibrahim. "Novel wideband microstrip monopole antenna designs for WiFi/LTE/WiMax devices." *IEEE Access* 8 (2020): 9532-9539. https://doi.org/10.1109/ACCESS.2019.2963644

[12] Dheyab, Ehab, and Nidal Qasem. "Design and optimization of rectangular microstrip patch array antenna using frequency selective surfaces for 60 GHz." *International Journal of Applied Engineering Research* 11, no. 7 (2016): 4679-4687.
[13] Kishore, Siddharth, and AR Abdul Rajak. "Microstrip patch antenna with C slot for 5G communication at 30 GHz." *Emerging Science Journal* 6, no. 6 (2022): 1315-1327. https://doi.org/10.28991/ESJ-2022-06-06-06
[14] Sree, Mohamed Fathy Abo, Wael Swelam, Mohamed Hassan, and Hadia El-Hennawy. "An inverted f with dual frequency for radar & 5g applications above 85 ghz." In *2019 PhotonIcs & Electromagnetics Research Symposium-Spring (PIERS-Spring)*, pp. 4152-4160. IEEE, 2019. https://doi.org/10.1109/PIERS-Spring46901.2019.9017523
[15] Emara, Hesham, Sherif El Dyasti, Hussein Ghouz, and Mohamed Abo Sree. "Design of a compact dual-frequency microstrip antenna using DGS structure for millimeter-wave applications." *Journal of Advanced Research in Applied Sciences and Engineering Technology* 28, no. 3 (2022): 221-234. https://doi.org/10.37934/araset.28.3.221234
[16] Ullah, Shahid, Cunjun Ruan, Muhammad Shahzad Sadiq, Tanveer Ul Haq, Ayesha Kosar Fahad, and Wenlong He. "Super wide band, defected ground structure (DGS), and stepped meander line antenna for WLAN/ISM/WiMAX/UWB and other wireless communication applications." *Sensors* 20, no. 6 (2020): 1735. https://doi.org/10.3390/s20061735
[17] Studio, CST Microwave. "CST, Framingham, MA, USA, 2012." (2018).
[18] Zhang, Huan Huan, Guo Guo Yu, Xin Zhi Liu, Guang Shang Cheng, Yun Xue Xu, Ying Liu, and Guang Ming Shi. "Low-SAR MIMO antenna array design using characteristic modes for 5G mobile phones." *IEEE Transactions on Antennas and Propagation* 70, no. 4 (2021): 3052-3057. https://doi.org/10.1109/TAP.2021.3121174
[19] Ye, Yang, Xing Zhao, and Junyin Wang. "Compact high-isolated MIMO antenna module with chip capacitive decoupler for 5G mobile terminals." *IEEE Antennas and Wireless Propagation Letters* 21, no. 5 (2022): 928-932. https://doi.org/10.1109/LAWP.2022.3152236
[20] Kiani, Saad Hassan, Amjad Iqbal, Sai-Wai Wong, Huseyin Serif Savci, Mohammad Alibakhshikenari, and Mariana Dalarsson. "Multiple elements MIMO antenna system with broadband operation for 5th generation smart phones." *IEEE Access* 10 (2022): 38446-38457. https://doi.org/10.1109/ACCESS.2022.3165049
[21] Alja'Afreh, Saqer S., Bayan Altarawneh, Mallak H. Alshamaileh, R. Almajali E'qab, Rifaqat Hussain, Mohammad S. Sharawi, Lei Xing, and Qian Xu. "Ten antenna array using a small footprint capacitive-coupled-shorted loop antenna for 3.5 GHz 5G smartphone applications." *IEEE Access* 9 (2021): 33796-33810. https://doi.org/10.1109/ACCESS.2021.3061640
[22] Ullah, Atta, Naser Ojaroudi Parchin, Mohamed Abdul-Al, Henrique MD Santos, Chan Hwang See, Yim Fun Hu, and Raed A. Abd-Alhameed. "Internal MIMO antenna design for multi-band mobile handset applications." In *2021 29th Telecommunications Forum (TELFOR)*, pp. 1-4. IEEE, 2021. https://doi.org/10.1109/TELFOR52709.2021.9653362
[23] Kiani, Saad Hassan, Ahsan Altaf, Muhammad Rizwan Anjum, Sharjeel Afridi, Zulfiqar Ali Arain, Sadia Anwar, Salahuddin Khan *et al.,* "MIMO antenna system for modern 5G handheld devices with healthcare and high rate delivery." *Sensors* 21, no. 21 (2021): 7415. https://doi.org/10.3390/s21217415
[24] Shi, Ce, and Yufa Sun. "A wideband six-port 5G MIMO mobile phone antenna." In *2021 International Conference on Microwave and Millimeter Wave Technology (ICMMT)*, pp. 1-3. IEEE, 2021. https://doi.org/10.1109/ICMMT52847.2021.9618030
[25] Abdullah, Mujeeb, Ahsan Altaf, Muhammad Rizwan Anjum, Zulfiqar Ali Arain, Abdul Aleem Jamali, Mohammad Alibakhshikenari, Francisco Falcone, and Ernesto Limiti. "Future smartphone: MIMO antenna system for 5G mobile terminals." *IEEE access* 9 (2021): 91593-91603. https://doi.org/10.1109/ACCESS.2021.3091304
[26] Muhsin, Muhannad Y., Ali J. Salim, and Jawad K. Ali. "An eight-element MIMO antenna system for 5G mobile handsets." In *2021 International Symposium on Networks, Computers and Communications (ISNCC)*, pp. 1-4. IEEE, 2021. https://doi.org/10.1109/ISNCC52172.2021.9615663
[27] Liu, Ying, Aidi Ren, Hu Liu, and Hanyang Wang. "Eight-port MIMO array using characteristic mode theory for 5G smartphone applications." *IEEE Access* 7 (2019): 45679-45692. https://doi.org/10.1109/ACCESS.2019.2909070
[28] Li, Yixin, Yong Luo, and Guangli Yang. "High-isolation 3.5 GHz eight-antenna MIMO array using balanced open-slot antenna element for 5G smartphones." *IEEE Transactions on Antennas and Propagation* 67, no. 6 (2019): 3820-3830. https://doi.org/10.1109/TAP.2019.2902751
[29] Parchin, Naser Ojaroudi, Yasir Ismael Abdulraheem Al-Yasir, Ammar H. Ali, Issa Elfergani, James M. Noras, Jonathan Rodriguez, and Raed A. Abd-Alhameed. "Eight-element dual-polarized MIMO slot antenna system for 5G smartphone applications." *IEEE access* 7 (2019): 15612-15622. https://doi.org/10.1109/ACCESS.2019.2893112
[30] Parchin, Naser Ojaroudi, Yasir IA Al-Yasir, James M. Noras, and Raed A. Abd-Alhameed. "Dual-polarized MIMO antenna array design using miniaturized self-complementary structures for 5G smartphone applications." In *2019 13th European Conference on Antennas and Propagation (EuCAP)*, pp. 1-4. IEEE, 2019.

[31] Zhao, Anping, and Zhouyou Ren. "Size reduction of self-isolated MIMO antenna system for 5G mobile phone applications." *IEEE Antennas and Wireless Propagation Letters* 18, no. 1 (2018): 152-156. https://doi.org/10.1109/LAWP.2018.2883428

[32] Zhao, Xing, Swee Ping Yeo, and Ling Chuen Ong. "Decoupling of inverted-F antennas with high-order modes of ground plane for 5G mobile MIMO platform." *IEEE Transactions on Antennas and Propagation* 66, no. 9 (2018): 4485-4495. https://doi.org/10.1109/TAP.2018.2851381

[33] Rao, Li-Yan, and Churng-Jou Tsai. "8-loop antenna array in the 5 inches size smartphone for 5G communication the 3.4 GHz-3.6 GHz band MIMO operation." In *2018 Progress in Electromagnetics Research Symposium (PIERS-Toyama)*, pp. 1995-1999. IEEE, 2018. https://doi.org/10.23919/PIERS.2018.8598072

[34] Li, Ming-Yang, Yong-Ling Ban, Zi-Qiang Xu, Jinhong Guo, and Zhe-Feng Yu. "Tri-polarized 12-antenna MIMO array for future 5G smartphone applications." *IEEE Access* 6 (2017): 6160-6170. https://doi.org/10.1109/ACCESS.2017.2781705

[35] Sun, Libin, Haigang Feng, Yue Li, and Zhijun Zhang. "Compact 5G MIMO mobile phone antennas with tightly arranged orthogonal-mode pairs." *IEEE Transactions on Antennas and Propagation* 66, no. 11 (2018): 6364-6369. https://doi.org/10.1109/TAP.2018.2864674